Available online at www.sciencedirect.com
ScienceDirect
Journal of Solid State Chemistry 179 (2006) 3893–3899
JOURNAL OF SOLID STATE CHEMISTRY
www.elsevier.com/locate/jssc

Synthesis and high-temperature thermoelectric properties of Ni and Ti substituted $LaCoO_3$

R. Robert[a], L. Bocher[a], M. Trottmann[a], A. Reller[b], A. Weidenkaff[a,*]

[a]*EMPA, Swiss Federal Laboratories for Materials Testing and Research, Solid State Chemistry and Catalysis, Ueberlandstr. 129, CH-8600 Duebendorf, Switzerland*
[b]*Solid State Chemistry, University of Augsburg, Germany*

Received 3 July 2006; received in revised form 18 August 2006; accepted 21 August 2006
Available online 24 August 2006

Abstract

The effect of Ti and Ni substitution in $LaCoO_{3-\delta}$ was investigated by means of electrical resistivity and Seebeck coefficient properties in a broad temperature range. The studied compounds crystallize in a rhombohedral crystal structure within the whole substitution range. The Seebeck coefficient of most of the studied compounds is positive indicating predominant hole-type charge carriers. The electrical resistivity decreases with increasing temperature for all compositions. Increasing the Ni content results in a decrease of the electrical resistivity, while the resistivity increases with increasing Ti content. The power factor, *PF*, for the Ni substituted samples is $PF = 1.42 \times 10^{-4}\,W/m^2\,K$ for $x = 0.10$ at $T = 540\,K$ and decreases with temperature. The $LaCo_{1-x}Ti_xO_{3\pm\delta}$ compounds reveal an enhancement of the power factor with increasing temperature. Ti substitution leads to a higher power factor compared to that of Ni substitution at $T = 1240\,K$.

Keywords: Thermopower; Perovskites; Transport properties; Cobaltates

1. Introduction

A large amount of the energy we use today comes from limited resources such as fossil fuels. The use of this energy releases polluting emissions into the atmosphere which generate unpredictable influences on our environment. Over the last 20 years there have been major steps in the development of renewable energy technologies for both industrial and domestic use. Intensive research is being done to improve the efficiency in the implementation of "green" energy sources such as solar power [1]. Solar energy can be directly converted into electrical energy by thermoelectric power generators [2]. Compared to photovoltaic technology, which is mostly limited to the UV-part of the solar radiation, thermoelectric devices can harvest energy from the whole solar radiation spectrum. The advantage of thermoelectric oxide modules (TOM) is the possibility to enlarge the operating range of temperature and thus the efficiency due to the high stability of oxides at high temperatures in air [3–5]. Furthermore, thermoelectric oxide devices can be realised on the basis of low cost materials with low toxicity. The scope of thermoelectricity applications depends on the thermoelectric energy conversion efficiency by means of the temperature difference over which the device is operating, and the so-called figure of merit, $Z = S^2/\rho\kappa$, where S is the Seebeck coefficient, ρ is the electrical resistivity and κ is the thermal conductivity. Operation at a temperature of $T = 1200\,K$, cold junction at $T = 300\,K$, shows a theoretical heat into electricity conversion efficiency, η, around 15% for a Z value of $0.001\,K^{-1}$ (see Fig. 1) calculated by the following equation[2]:

$$\eta = \frac{T_H - T_C}{T_H} \times \left(\frac{(\sqrt{1+ZT}) - 1}{(\sqrt{1+ZT})(T_H/T_C)} \right), \quad (1)$$

where T_H and T_C are the temperature at the hot and cold junction, respectively, T is the average of the T_H and T_C, Z is the dimensionless figure of merit of the thermoelectric couple.

*Corresponding author. Fax: +41 1 823 40 41.
E-mail address: anke.weidenkaff@empa.ch (A. Weidenkaff).

0022-4596/$ - see front matter © 2006 Elsevier Inc. All rights reserved.
doi:10.1016/j.jssc.2006.08.022

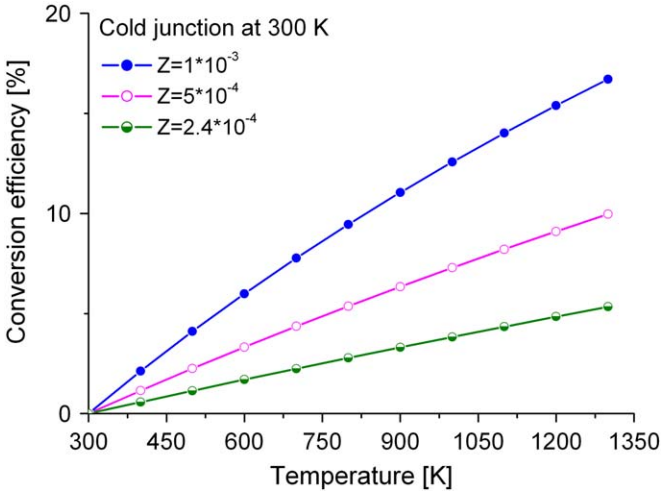

Fig. 1. Conversion efficiency η of a thermoelectric converter as function of the temperature gradient for different Z values.

The state-of the-art thermoelectric oxide materials display a figure of merit value, ZT, around unity, e.g. Na_xCoO_3 single crystal shows a $Z = 0.001\,K^{-1}$ at $T = 800\,K$ ($ZT = 0.8$) [6] and the $(Na_xCa_{1-x})_3Co_4O_9$ compound exhibit a $Z = 1.2{*}10^{-4}\,K^{-1}$ at $T = 973\,K$ ($ZT = 1.2$) [7]. This ZT values would show a conversion efficiency values of $\eta = 9.5$ at $T = 800\,K$ and $\eta = 14\%$ at $T = 973\,K$ respectively. An increase in temperature difference provides a corresponding increase of the Carnot efficiency. Therefore, large temperature differences are desirable and the evaluation of high-temperature thermoelectric properties is required. The largest ZT value up to now reported for oxides materials at high temperatures belongs to the $Zn_{0.98}Al_{0.02}O$ with $Z = 0.24 \times 10^{-3}\,K^{-1}$ and hence a $ZT = 0.30$ at $T = 1273\,K$ would give a conversion efficiency value of $\eta = 5.4\%$ [8].

Therefore, essential efficiency improvement requires the development of novel functional materials with enhanced figure of merit, Z [3,9] and high temperature stability, $T \geqslant 1400\,K$.

Intensive research is carried out on finding novel transition metal oxide thermoelectrics [10–13] exhibiting a large Seebeck coefficient S, a low electrical resistivity ρ and a low thermal conductivity κ in order to realize an efficient conversion of thermal energy into electrical energy. Among them, particularly cobalt oxides have attracted increasing attention for thermoelectric applications owing to the fact that they exhibit semiconducting or metallic electric conductivity and a large Seebeck coefficient [10,12,14].

Effects of cobalt site and lanthanum site substitution on the properties of perovskite-type cobaltates have been of great interest to the community (see [9,11,12,15–18]). The different substitutions in the cobaltates may considerably improve its transport properties by changing the oxidation state of cobalt. p- and n-type cobaltates can be designed by suitable substitutions, e.g. a low content of Ti^{4+} or Ce^{4+} changes the sign of the Seebeck coefficient to negative values [19,20].

The effect of Ni substitution into the $LaCoO_3$ system has been previously studied. Kobayashi et al. [21] studied the magnetic and transport properties of the $LaCo_{1-x}Ni_xO_3$ ($x = 0.05$, 0.1) single crystals at low-temperature and Rao et al. [22] reported electrical resistivity and susceptibility data of $LaCo_{1-x}Ni_xO_3$ ($x \leqslant 0.5$) up to $T = 1000\,K$. The temperature dependence of the electrical resistivity in the low temperature range, $T < 300\,K$, for compositions with $x = 0.2$, 0.3 and 0.7 nickel content was also investigated [23]. Recently, Migiakis et al. reported a figure of merit of $ZT = 0.022$ for $LaCo_{0.80}Ni_{0.20}O_3$ which is comparable to that of single crystalline $NaCo_2O_4$ ($ZT = 0.03$) at room temperature [10]. However, thermoelectric properties on this system at high temperature have not yet been reported.

The optimization of the figure of merit ($Z = S^2/\rho\kappa$) is still a challenge to be solved taking into account that S, σ and κ are interdependent. Large Seebeck coefficient values might be kept for a low substitution level and the thermal conductivity might be reduced by boundary scattering without affecting the electrical transport [24,25], e.g. a figure of merit of $ZT = 0.2$ for $LaCo_{0.80}Ni_{0.20}O_{2.95}$ is achieved at room temperature by decreasing the thermal conductivity to $\kappa = 0.5\,W/m\,K$ [26].

In this experimental study, the influence of partially substitution of the Co-site by Ti and Ni in the $LaCoO_3$ system is investigated by evaluating the electrical resistivity and the Seebeck coefficient up to $T = 1240\,K$. The power factor ($PF = S^2/\rho$) values up to $T = 1240\,K$ are reported. The perovskite-type oxides are synthesised by a soft chemistry method based on the chelation of metals with citric acid in aqueous solution. Lower reaction temperature ($T = 873\,K$) and two times shorter reaction cycles compared to ceramic methods allow the production of single phase metal oxides with various compositions and mesoporous morphology [27–29].

2. Experimental

Fine powders with the composition $LaCo_{1-x}Ni_xO_{3-\delta}$, (with $x = 0$, 0.02, 0.10 and 0.20) and $LaCo_{1-x}Ti_xO_{3\pm\delta}$ (with $x = 0.01$, 0.10 and 0.20) were obtained by thermal decomposition of the corresponding amorphous citrate precursors [26]. The formation of the perovskite phase from water soluble precursors is described in detail in former publications (see [9,28,29]). The precursors for the $LaCo_{1-x}Ni_xO_{3-\delta}$ compositions were prepared from an aqueous solution containing stoichiometric amounts of dissolved $La(NO_3)_3 \times 6H_2O$ (Merck, $\geqslant 97\%$), $Co(NO_3)_2 \times 6H_2O$ (Merck, $\geqslant 97\%$) and $Ni(NO_3)_2 \times 6H_2O$ (Merck, $\geqslant 99\%$). An excess of the chelating agent, citric acid (Sigma-Aldrich), was added to the metal salt solution under continuous stirring at room temperature in order to prevent precipitation. The citric acid to metal ion ratio was 2:1. Homogeneous clear solutions were obtained after heating and polymerization under reflux for 3 h at $T = 553\,K$. The precursor solution was dried using a rotary evaporator ($T = 333\,K$, $p = 20\,mbar$) to promote

the formation of a pink-transparent viscous gel. The gel was pre-decomposed at $T = 573$ K resulting in a voluminous product which was then milled and calcinated at $T = 873$ K in ambient atmosphere for 4 h to obtain the $LaCo_{1-x}Ni_xO_{3-\delta}$ phases.

The precursor solution for the $LaCo_{1-x}Ti_xO_{3\pm\delta}$ compositions was prepared in two steps. Titanium metal (Alfa) was dissolved in hydrogen peroxide aqueous solution (Merck) and ammonia hydroxide aqueous solution (Merck) to produce a water soluble peroxytitanium complex [30]. A clear yellow solution with pH = 11 was developed under stirring for aprox. 3 h. Citric acid was added to the peroxytitanium complex solution in order to stabilise the citrato-peroxo-titanate-precursor. The pH of the citrate peroxytitanium complex solution was adjusted to pH = 5. An aqueous solution consisting of $La(NO_3)_3 \times 6H_2O$, $Co(NO_3)_2 \times 4H_2O$ and citric acid was added to the citrate peroxytitanium complex solution, resulting in an orange clear solution. The viscous and intense orange solutions were dried in the furnace at $T = 373$ K resulting in a brown resin. The resin was pre-decomposed at $T = 573$ K which was then milled and calcinated at $T = 873$ K in ambient atmosphere for 4 h to obtain the $LaCo_{1-x}Ti_xO_{3\pm\delta}$ (with $x = 0.01$, 0.10 and 0.20) phases.

The thermal decomposition of the different precursors was analyzed by thermogravimetric analysis (TGA) using a Netzsch STA 409 CD system coupled to a Netzsch QMS 403 C Aëolos mass spectrometer. The amorphous citrate precursors were heated to $T = 1273$ K in a gas atmosphere of 80% helium and 20% oxygen with a heating rate of 2 K/min. Thermogravimetric (TG) and a differential thermal analytical (DTA) signals were recorded as a function of temperature.

The structural analysis of the products was done using X-ray diffraction (XRD) and neutron diffraction (ND). X-ray diffraction data were collected with a PANanalytical X'pert diffractometer with Cu$K\alpha$ radiation. Neutron diffraction data were recorded on the High-Resolution Powder Diffractometer for Thermal Neutrons (HRPT) of the Swiss Neutron Spallation Source (SINQ) in a temperature range of $1.5\,K < T < 700$ K. The morphology of the calcinated product powders was analyzed using a LEO JSM-6300F scanning electron microscope (SEM) and a Phillips CM30 transmission electron microscope (TEM). The surface area was measured with a Quantachrome 3000 CHEMBET by applying the BET-method.

The cationic composition was analysed for all samples by Rutherford Backscattering Spectrometry (RBS). Measurements were performed using a 2 MeV 4He beam and a silicon surface barrier detector under 165°. The collected data were evaluated using the RUMP program [31]. The oxygen content was analysed by the hot gas extraction method using a LECO TC 500.

The electrical transport property measurements were done on bar-shaped pressed pellets with dimensions of 1.65 mm × 5–10 mm × 1 mm sintered at $T = 1373$ K in air. The electrical resistivity was measured using a Quantum Design Physical Properties Measurement System (PPMS) in the temperature range of $4\,K < T < 350$ K by the four contact method with indium contacts. In the high-temperature range ($340\,K < T < 1240$ K) the electrical conductivity and the Seebeck coefficient were measured using the RZ2001i measurement system from Ozawa science, Japan. The electrical conductivity and the Seebeck coefficient were measured simultaneously as a function of temperature. The Seebeck coefficient was measured by steady-state method and the electrical conductivity was measured by the DC four-probe method. Two electrical contacts were placed at the ends of the sample and the two others on the sample body. The contacts at the ends were made mechanically with Pt layers. The contacts on the body were made by surrounding the bar-shaped sample with Pt wires.

3. Results and discussion

Ti and Ni substituted lanthanum cobaltate compounds adopting the perovskite structure were synthesized by the citric acid-complexation method. Thermogravimetric analyses were performed for compounds with various compositions [26,32]. The decomposition of the Ni substituted amorphous citrate precursors was analysed by means of the weight loss (TG) and differential thermal analysis (DTA) as a function of temperature (not shown here). Below $T = 438$ K a weak endothermic process with a weight loss of 3 mass% is monitored, which corresponds to the release of H_2O as found by the on-line MS signal (m/z 18). Thermal degradations observed in the temperature range of $463\,K < T < 613$ K are due to the thermal decomposition of the organic network. At $T \sim 463$ K citric acid is released which can be concluded from MS signals of the citric acid fragments, $C_2H_2O_2^+$ (m/z 58), $C_3H_3^+$ (m/z 39) and $C_4H_4O^+$ (m/z 68). At $T \sim 578$ K the organic network further decomposes leading to water and carbon oxide emissions, CO_2 (m/z 44), CO (m/z 28). The differential thermal analysis data reveal an exothermic event corresponding to a weight loss of 25 wt%. In this temperature range ($T \sim 578$ K) the perovskite-type metal oxide starts to form. The TGA study reveals no further weight change up to $T > 823$ K which indicates that the formation of the pure transition metal oxide is completed. Further heating to $T = 1273$ K does not reveal any weight or energetic changes in the corresponding TG and DTA signal. Thus, it can be concluded that the metal oxide remains stable up to $T = 1273$ K which is confirmed by XRD as well as by ND data. The morphology studies on the powders heated at $T = 873$ K reveal a porous structure. The particles with an uniform particle size of approximately 70 nm diameter are partly agglomerated (see Fig. 2a and b). The powders exhibit typically a BET-surface area of 16–18 m^2/g. After further annealing at $T = 1273$ K, the sintering processes lead to an increase of the crystallite size to a submicrometer level. Accordingly, the surface area is reduced to nearly

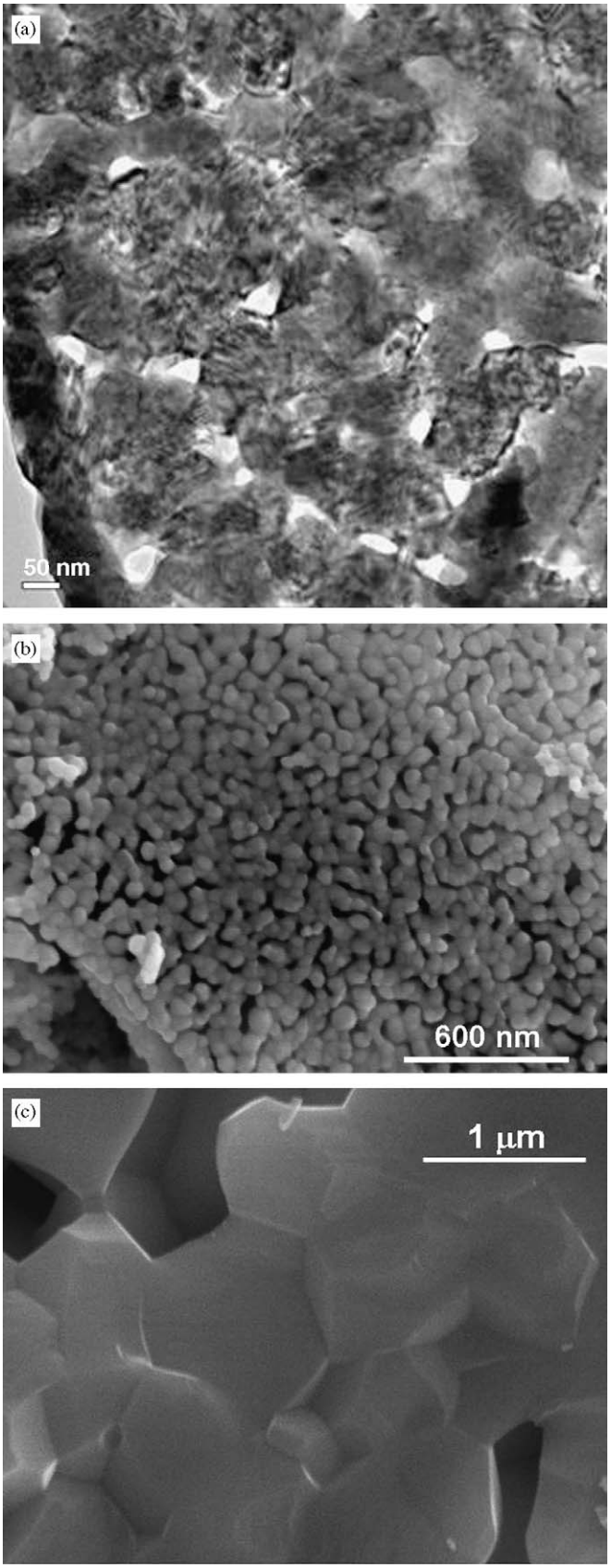

Fig. 2. TEM and SEM micrograph pictures of powders with the composition $LaCo_{0.90}Ni_{0.10}O_{2.92}$ produced at $T = 873$ K (a, b), and $T = 1273$ K (c).

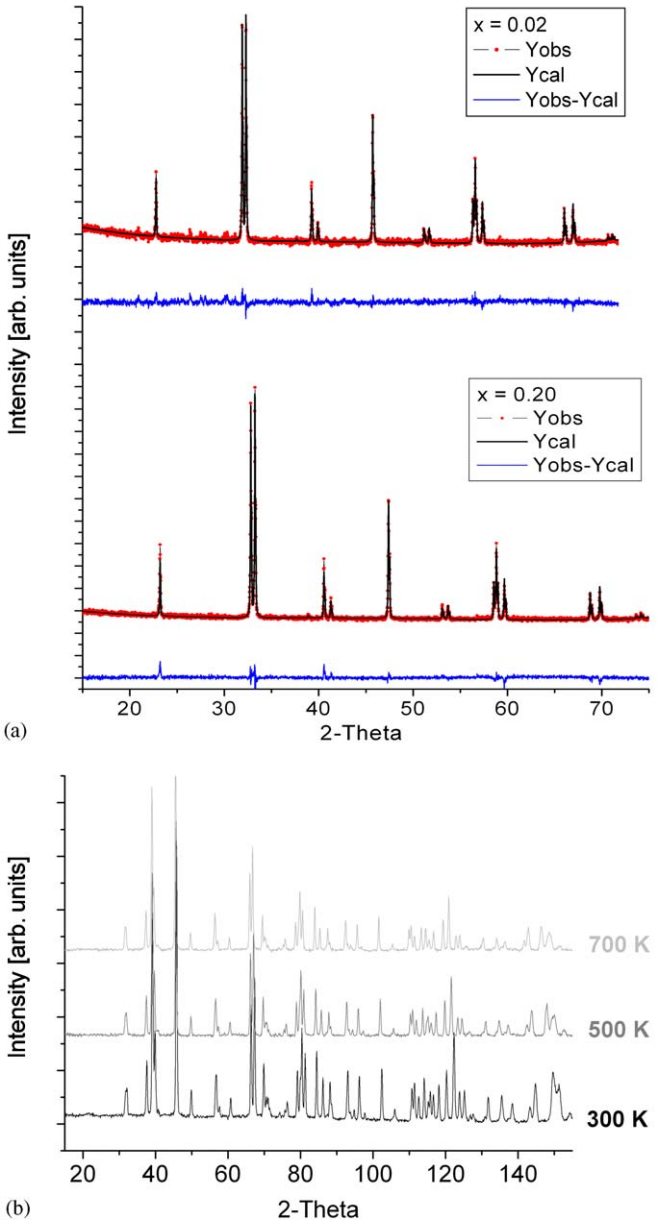

Fig. 3. Rietveld refinement plot (black line, Y_{cal}) of the X-ray powder diffraction data for $LaCo_{1-x}Ni_xO_{3-\delta}$ ($x = 0.02$ and 0.20) compounds at room temperature (red points, Y_{obs}). The bars indicate the allowed Bragg reflections. The difference curve between observed and calculated profiles is plotted at the bottom (blue line), (a) and the ND data of $LaCo_{0.92}Ni_{0.08}O_{2.95}$ at different temperatures (b).

$1\,m^2/g$. Fig. 2c shows the typical morphology of the powders when sintered at high temperature. The nominal cationic composition was confirmed by Rutherford Backscattering Spectrometry with an accuracy of more than 96%. Hot-gas extraction results indicate that all the Ni-substituted samples were slightly oxygen deficient. The resulting oxygen deficiencies of $LaCo_{1-x}Ni_xO_{3-\delta}$ are $\delta = 0.05 \pm 0.03$ for $x = 0.02$, $\delta = 0.08 \pm 0.02$ for $x = 0.10$, and $\delta = 0.05 \pm 0.03$ for $x = 0.20$. The oxygen non-stoichiometries of $LaCo_{1-x}Ti_xO_{3\pm\delta}$ are $\delta = 0.07 \pm 0.07$ for $x = 0.01$,

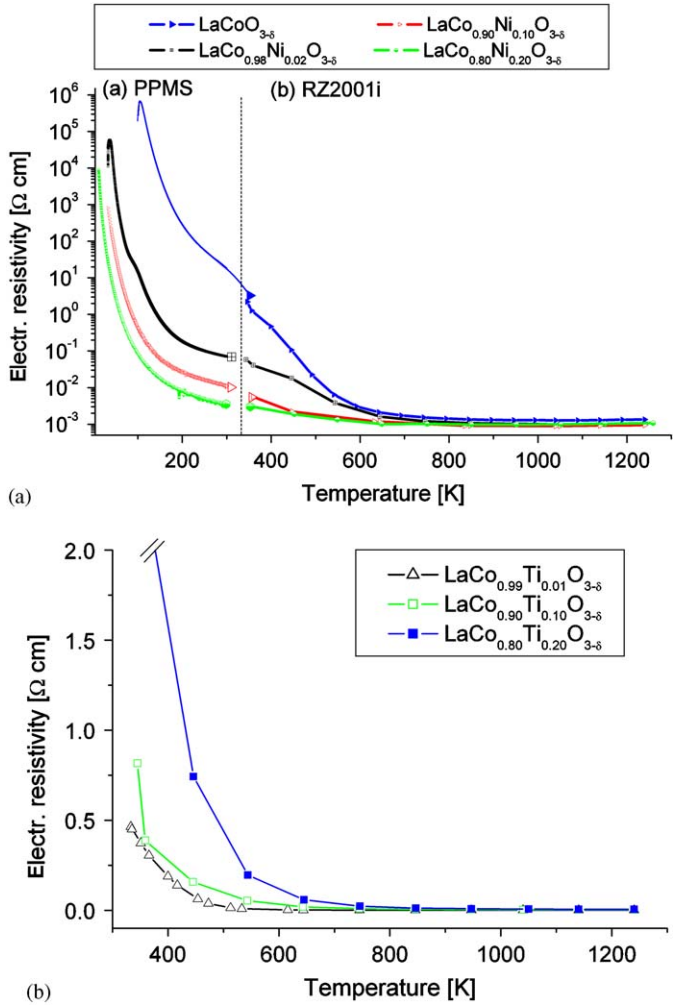

Fig. 4. Temperature dependence of the electrical resistivity of $LaCo_{1-x}Ni_xO_{3-\delta}$ ($x = 0$, 0.02, 0.10, and 0.20) in the temperature range of $20\,K < T < 1273\,K$ (a), and temperature dependence of the electrical resistivity of $LaCo_{1-x}Ti_xO_{3\pm\delta}$ ($x = 0.01$, 0.10, and 0.20) in the temperature range of $340\,K < T < 1240\,K$ (b).

$\delta = 0.03 \pm 0.02$ for $x = 0.10$, and $\delta = 0.14 \pm 0.07$ for $x = 0.20$.

Powder X-ray diffraction data reveal that all samples are single-phase and crystallize in the rhombohedral crystal symmetry (space group $R3c$). X-ray diffraction patterns (see Fig. 3a), recorded at room temperature were used to determine the lattice parameters and the theoretical density depending on the Ni substitution. According to neutron diffraction results, there is no evidence of a structural phase transition while heating up to $T = 700\,K$ (see Fig. 3b). The stability of the pure perovskite phase was confirmed by thermoanalytic experiments up to $T = 1273\,K$.

In Fig. 4a the temperature dependence of the electrical resistivity of $LaCo_{1-x}Ni_xO_{3-\delta}$ (with $x = 0$, 0.02, 0.10, and 0.20) compounds in the temperature range of $20\,K < T < 1240\,K$ is displayed. The electrical resistivity decreases with increasing temperature ($d\rho/dT < 0$), representing a semiconductor-type behaviour for all the studied compositions. 2% Ni ions substitution in the cobaltate structure induces a high decrease of the electrical resistivity from $\rho = 17.5\,\Omega cm$ to $\rho = 70.8\,m\Omega cm$ at $T = 300\,K$. Further increase of Ni substitution, $x = 0.20$, leads to a decrease of the electrical resistivity value to $\rho = 3.5\,m\Omega cm$ which is close to the reported value of $\rho = 9.6\,m\Omega cm$ at room temperature [23]. The decrease of electrical resistivity with increasing nickel content is in good agreement with the reported low temperature data [21,23]. The decrease of the electrical resistivity by the introduction of nickel into the cobalt sublattice has been attributed to an increasing mobility of the itinerant σ^* electrons in the narrow Ni^{III}-σ^* impurity bands [23]. The effect of decreasing the electrical resistivity with increasing nickel content can also be associated to an increase of Co^{4+} and thus the number of positive charge carriers in the mixed valence band [11]. In the $LaCo_{1-x}Ni_xO_{3-\delta}$ system, the Co^{4+} formation is induced by the substitution of the Co^{3+} by Ni^{2+} ions [21]. At $T > 800\,K$ all compounds show a similar low electrical resistivity in the range of $0.89\,m\Omega cm < \rho < 1.13\,m\Omega cm$. This feature remains fairly constant up to $T = 1240\,K$. The

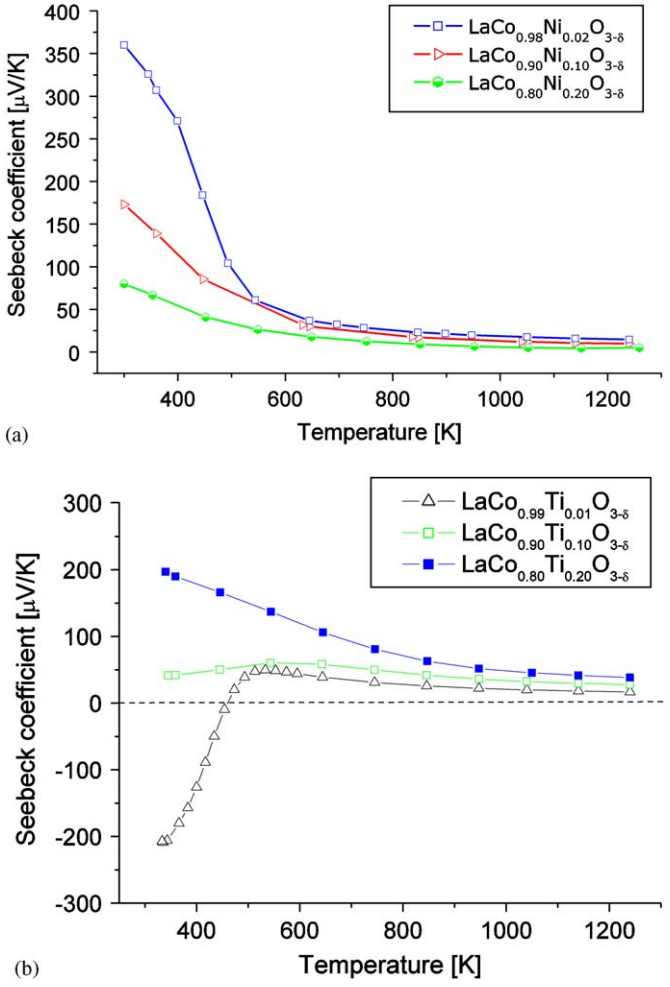

Fig. 5. Temperature dependence of the Seebeck coefficient of $LaCo_{1-x}Ni_xO_{3-\delta}$ ($x = 0.0$, 0.02, 0.08, and 0.20) in the range of $300\,K < T < 1240\,K$, (a) and temperature dependence of the Seebeck coefficient of $LaCo_{1-x}Ti_xO_{3\pm\delta}$ ($x = 0.01$, 0.10, and 0.20) in the range of $340\,K < T < 1240\,K$ (b).

electrical resistivity measurements of $LaCo_{1-x}Ti_xO_{3-\delta}$ ($0.01 \leqslant x \leqslant 0.20$) vs. temperature are depicted in Fig. 4b. All samples reveal a semiconducting-like behaviour up to $T = 1240\,K$. The electrical resistivity increases dramatically with increasing Ti content, which induces the formation of Co^{2+} ions. The high resistivity is due to the fact that the transport takes place in the e_g band of the 3d orbital for Co^{2+}/Co^{3+}, and the hopping in the e_g band is not possible by moving only one electron [33].

The Seebeck coefficient has been measured in the temperature range of $300\,K < T < 1240\,K$ (see Fig. 5a). The Seebeck coefficient is positive indicating predominant positive mobile charge carriers for all the Ni-substituted compositions. The substitution of Co by Ni in the $LaCo_{1-x}Ni_xO_{3-\delta}$ system increases the charge carrier concentration leading to a reduction of the absolute Seebeck coefficient value at room temperature following Heikes equation [34]. The effect of 2% of Ni substitution in the $LaCoO_3$ compound reduces the Seebeck coefficient from $S = +600\,\mu V/K$ (for the non-substituted p-type $LaCoO_3$) to $S = +360\,\mu V/K$. Assuming that for the compositions with nickel content of $x \leqslant 0.10$ the electrical conduction is generated by a hopping mechanism and the Seebeck coefficient is slightly temperature dependent up to $T = 300\,K$ [21], the Seebeck coefficient at room temperature can be estimated by using the temperature-independent thermoelectric power described by Heikes equation [34,35]:

$$S = -\frac{k_B}{e}\ln\left(\frac{x}{1-x}\right), \tag{2}$$

where k is the Boltzmann's constant, and x is the fraction of Co site occupied by a charge carrier.

Applying this formula, e.g. for $x = 0.02$ the theoretical Seebeck coefficient reaches a value of $S_{Heikes} = +335\,\mu V/K$ which is in good approximation with the experimental value, $S_{exp(300\,K)} = +360\,\mu V/K$. For $x = 0.10$ the theoretical Seebeck coefficient adopts a value of $S_{Heikes} = +189\,\mu V/K$ which corresponds to $S_{exp(300\,K)} = +173\,\mu V/K$ at room temperature. For an $x \geqslant 0.20$ the $LaCo_{1-x}Ni_xO_{3-\delta}$ becomes metallic and thus the Seebeck coefficient does not follow Heikes equation. The increase of the temperature leads to a decrease of the Seebeck coefficient at $T > 300\,K$. This broad transition is also observed in the electrical resistivity, see Fig. 4a. In the $LaCoO_3$ compound the Co^{3+} ion can be found in three different spin states. At low temperatures the Co^{3+} ions adopt the low spin state ($t_{2g}^6 e_g^0$). With increasing temperature, the Co^{3+} ions in the low spin state undergo a transition to an intermediate spin state ($t_{2g}^5 e_g^1$), and to a high spin state configuration ($t_{2g}^4 e_g^2$) at $T = 1200\,K$ [36]. Such transitions seem to be related to the observed change of transport properties with temperature. At $T > 800\,K$, the Seebeck coefficient slightly decreases, $S_{(x=0.02)} = +14.7\,\mu V/K$ and $S_{(x=0.10)} = +9.7\,\mu V/K$ at $T = 1240\,K$. The behaviour of the Seebeck coefficient at high temperature has been explained as a consequence of the disproportionation of Co^{3+} ions into $Co^{4+} + Co^{2+}$ pairs in the $LaCoO_3$ system [37]. For the sample with the composition $LaCo_{1-x}Ni_xO_{3-\delta}$ ($x = 0.02$ and 0.10) the Seebeck coefficient adopts a similar value of $S = +12\,\mu V/K$ at $T = 1240\,K$. In Fig. 5b the Seebeck coefficient for $LaCo_{1-x}Ti_xO_{3\pm\delta}$ ($x = 0.01$, 0.10, and 0.20) compounds is shown. A negative thermoelectric power is found in low level substituted $LaCo0.99Ti_{0.01}O_{3.07}$. When Co^{3+} ions are substituted by Ti^{4+} ions in the $LaCoO_3$ system, Co^{2+} ions are generated, and negative charge carriers are introduced into the system. At low substitution level, two types of charge carriers may be present, but electrons are dominating at room temperature leading to a large negative Seebeck coefficient. $LaCo_{0.99}Ti_{0.01}O_{3.07}$ and $LaCo_{0.90}Ti_{0.10}O_{0.97}$ compounds exhibit the same temperature dependence of the Seebeck coefficient. The S increases with increasing temperature up to $T = 550\,K$. Above $T = 550\,K$, the Seebeck coefficient decreases with increasing temperature. For the compositions with Ti content of $x = 0.10$ and 0.20, the Seebeck coefficient is positive in the whole temperature range.

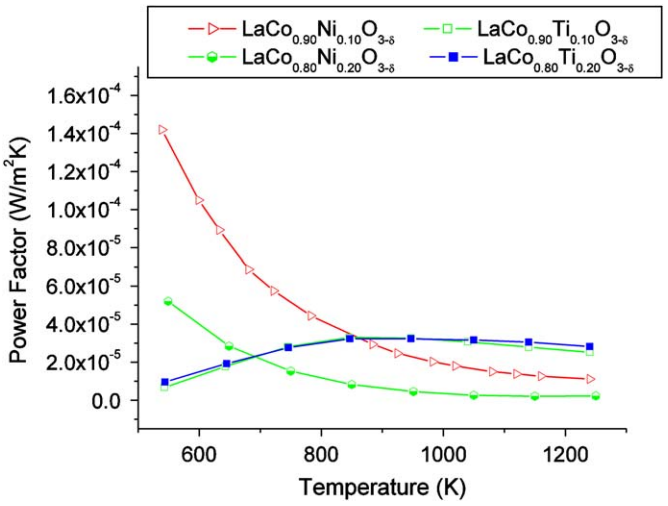

Fig. 6. Temperature dependence of the power factor of $La Co_{1-x}(Ti,Ni)_xO_{3\pm\delta}$ (with $x = 0.10$, and 0.20) in the temperature range of $500\,K < T < 1240\,K$.

The PF of the Ni-substituted compounds decreases with increasing temperature. However, the compound with $x = 0.10$ nickel content has a $PF = 1.42 \times 10^{-4}\,W/m^2\,K$ at $T = 540\,K$. On the other hand, the Ti substituted compounds exhibit an increase of the power factor with increasing temperature (see Fig. 6). Ti substitution leads to higher PF at $T = 1240\,K$ compared to that of Ni substituted compounds, e.g. $PF(LaCo_{0.80}Ti_{0.20}O_{2.86}) = 2.82 \times 10^{-5}\,W/m^2\,K$ and $PF(LaCo_{0.80}Ni_{0.20}O_{2.95}) = 9.5 \times 10^{-6}\,W/m^2\,K$ at $T = 1240\,K$.

4. Conclusions

A series of single phase powders with a nominal composition of $LaCo_{1-x}Ni_xO_{3-\delta}$, ($0.02 \leqslant x \leqslant 0.20$), and $LaCo_{1-x}Ti_xO_{3\pm\delta}$, (0.01, 0.10, and 0.20) were prepared by

a soft-chemistry process. Pure phases were obtained at relatively low temperature, i.e. at $T = 873\,K$. X-ray diffraction analyses on crystalline samples reveal that all samples crystallize with rhombohedral crystal symmetry (space group $R3c$). Thermogravimetric experiments and neutron diffraction data gave no evidence for a crystallographic phase transition up to $T = 700\,K$. The electrical conductivity and the Seebeck coefficient were measured in a broad temperature range. The electrical resistivity decreases with increasing Ni content. The electrical resistivity increases considerably with increasing Ti content. The Seebeck coefficient decreases with increasing Ni content and with increasing temperature. For 1% Ti substituted $LaCoO_3$, negative charge carriers are dominating and leading to a large negative Seebeck coefficient of $S = -200\,\mu V/K$ at 340 K. Ti substitution leads to higher PF values compare to that of Ni substituted compounds at high temperature, $T > 900\,K$.

The Ti substituted LaCo oxides were found to be of great interest as high temperature thermoelectric materials since the PF increases with temperature.

Acknowledgments

The authors thank Max Döbeli, ETHZ, for RBS measurements, R. Figi, Empa, for helping to perform oxygen content determination, and the Swiss Federal Office of Energy for financial support.

References

[1] A. Steinfeld, Sol. Energy 78 (2005) 603–615.
[2] D.M. Rowe, General principles and basic considerations, in: D.M. Rowe (Ed.), Thermoelectrics Handbook, Taylor & Francis Group, London, 2006 Chap. 1.
[3] I. Matsubara, R. Funahashi, T. Takeuchi, S. Sodeoka, T. Shimizu, K. Ueno, Appl. Phys. Lett. 78 (2001) 3627–3629.
[4] R.E. Sudhakar, J.G. Noudem, S. Hébert, C. Goupil, J. Phys. D: Appl. Phys. 38 (2005) 3751–3755.
[5] R. Funahashi, M. Mikami, T. Mihara, S. Urata, N. Ando, J. Appl. Phys. 99 (2006) 066117.
[6] M. Ito, T. Nagira, D. Furumoto, S. Katsuyama, H. Nagai, Scr. Mater. 48 (2003) 403–408.
[7] M. Shikano, R. Funahashi, Appl. Phys. Lett. 82 (2003) 1851–1853.
[8] K. Koumoto, I. Terasaki, T. Kajitani, M. Ohtaki, R. Funahashi, Oxide Thermoelectrics, in: D.M. Rowe (Ed.), Thermoelectrics handbook, Taylor & Francis Group, London, 2006 Chap. 35.
[9] R. Robert, S. Romer, A. Reller, A. Weidenkaff, Adv. Eng. Mater. 7 (2005) 303–308.
[10] I. Terasaki, Y. Sasago, K. Uchinokura, Phys. Rev. B: Condens. Matter 56 (1997) R12685–R12687.
[11] S. Hébert, D. Pelloquin, C. Martin, A. Maignan, Cobalt Oxides as potential thermoelectric elements: The influence of the Dimensionality. 22nd International Conference on Thermoelectrics, 2003, pp. 161–166.
[12] A. Maignan, S. Hébert, L. Pi, D. Pelloquin, C. Martin, C. Michel, M. Hervieu, B. Raveau, Cryst. Eng. 5 (2002) 365–382.
[13] J. Hejtmánek, Z. Jirák, D. Sedmidubský, A. Maignan, C. Simon, V. Caignaert, C. Martin, B. Raveau, Phys. Rev. B: Condens. Matter 53 (1996) 11947–11950.
[14] A. Maignan, L.B. Wang, S. Hébert, D. Pelloquin, B. Raveau, Chem. Mater. 14 (2002) 1231–1235.
[15] T. Ohtani, K. Kuroda, K. Matsugami, D. Katoh, J. Eur. Ceram. Soc. 20 (2000) 2721–2726.
[16] D. Pelloquin, S. Hébert, A. Maignan, B. Raveau, J. Solid State Chem. 178 (2005) 769–775.
[17] V. Morchshakov, L. Haupt, K. Barner, I.O. Troyanchuk, G.H. Rao, A. Ghoshray, E. Gmelin, J. Alloys Compd. 372 (2004) 17–24.
[18] Y. Kobayashi, T. Nakajima, K. Asai, J. Magn. Magn. Mater. 272–276 (2004) 83–84.
[19] S. Hébert, D. Flahaut, M. Miclau, V. Caignaert, C. Martin, D. Pelloquin, A. Maignan, Search for New n-type Thermoelectric Oxides. 8th European Workshop on Thermoelectrics, (2004).
[20] A. Maignan, D. Flahaut, S. Hébert, Eur. Phys. J. B 39 (2004) 145–148.
[21] Y. Kobayashi, S. Murata, K. Asai, J.M. Tranquada, G. Shirane, K. Kohn, J. Phys. Soc. Japan 68 (1999) 1011–1017.
[22] C.N.R. Rao, O. Parakash, P. Ganguly, J. Solid State Chem. 15 (1975) 186–192.
[23] P. Migiakis, J. Androulakis, J. Giapintzakis, J. Appl. Phys. 94 (2003) 7616–7620.
[24] R. Robert, S. Romer, S. Hébert, A. Maignan, A. Weidenkaff, Proccedings of the 8th European Workshop on Thermoelectrics, 2004.
[25] P. Heitjahns, S. Indris, J. Phys. 15 (2003) R1257–R1289.
[26] R. Robert, L. Bocher, B. Sipos, M. Döbeli, A. Weidenkaff, Prog. Solid State Chem. (2006) (in press).
[27] F.S. Galasso, Structure, Properties and Preparation of Perovskite-type Compounds, Pergamon Press, New York, 1969.
[28] E. Krupicka, A. Reller, A. Weidenkaff, Cryst. Eng. 5 (2002) 195–202.
[29] A. Weidenkaff, Adv. Eng. Mater. 6 (2004) 709.
[30] E.R. Camargo, M. Popa, J. Frantti, M. Kakihana, Chem. Mater. 13 (2001) 3943–3948.
[31] L. R. Doolittle, Simulation Programm RUMP, 1985.
[32] L. Bocher, M. H. Aguirre, R. Robert, M. Trottmann, D. Logvinovich, P. Hug, A. Weidenkaff, PCCP, 2006, to be submitted.
[33] A. Maignan, V. Caignaert, B. Raveau, D. Khomskii, G. Sawatzky, Phys. Rev. Lett. 93 (2004) 026401.
[34] R.R. Heikes, R.C. Miller, R. Mazelsky, Physica B 30 (1964) 1600–1608.
[35] J.-S. Zhou, J.B. Goodenough, Phys. Rev. B: Condens. Matter 60 (1999) R15002–R15004.
[36] M.A. Señarís-Rodríguez, J.B. Goodenough, J. Solid State Chem. 118 (1995) 323–336.
[37] C. Autret, J. Hejtmánek, K. Knížek, M. Maryško, Z. ZJirák, M. Dlouhá, S. Vratislav, J. Phys.: Condens. Matter 17 (2005) 1601–1616.